Effect of liquid flow rate and bed void fraction on the hydrodynamics and performance of a trickle-bed bioreactor

Martín Cruz-Díaz [a,b], Sergio Revah[a], Ricardo Lobo-Oehmichen[a *]

[a] *Departamento de Ingeniería de Procesos e Hidráulica, Universidad Autónoma Metropolitana-Iztapalapa. San Rafael Atlixco 186, C.P. 09340, México, D.F., MEXICO*
[b] *División de Química y Bioquímica, Tecnologico de Estudios Superiores de Ecatepec, Av. Tecnologico S/N Esq. Av. Hank González, Valle de Anahuac, C.P. 55120, Ecatepec, Edo. de Mex, MEXICO*

Abstract

Hydrodynamics has a strong influence on substrate elimination capacity in trickle-bed bioreactors (TBB). The present study reports the influence of liquid mass flow rate and bed void fraction on the TBB liquid residence time distribution (RTD), gas-liquid pressure drop, liquid hold-up, and biofilm wetting efficiency. Most RTD are well represented by a dispersion model. It is also shown that the hydrodynamic parameters increase as superficial liquid mass flow rate increases and as bed void fraction diminishes. The TBB isopropyl alcohol (IPA) mineralization capacity reach its largest values at a bed void fraction of 0.6, and the lowest are obtained when it is 0.44, when the TBB turns anaerobic due to excessive biomass growth. Overall, it is shown that the TBB performance is strongly dependent on hydrodynamics.

Keywords: trickle-bed bioreactor, hydrodynamics, residence time distribution

1. Introduction

Trickle-bed bioreactors (TBB) have shown to be an effective technology for low concentration volatile organic compound (VOC) emissions control. TBB pollutant elimination capacity is determined by the characteristics of the microorganisms present in the supported biofilm and by the hydrodynamics of the flowing phases. The fluids mixing pattern, the gas and liquid flow regime, gas-liquid pressure drop, liquid hold-up, and wetting efficiency are particularly important for substrate and oxygen mass transfer from the gas to the liquid, and from the liquid to the biofilm, where the final removal of the pollutants take place. At the same time, the biofilm growth and its pollutant removal efficiency are determined by the supply of substrates, oxygen and other nutrients (Lobo et al., 1999; Cox and Deshusses, 2002). Although there is a large amount of literature on the effect of hydrodynamics on the behavior of chemical trickle bed reactors, little attention has been paid to TBB for VOC removal. In a xylene-removing TBB Trejo-Aguilar et al. (2005) showed that liquid flow deviated considerably from plug flow, depending on liquid mass rate and the amount of

* Corresponding author. lobo@xanum.uam.mx

biomass present en the reactor. They also presented quantitative data on gas-liquid pressure drop and liquid hold-up, showing that the magnitude of these parameters was strongly dependent on liquid mass rate and bed void fraction, and that these parameters had a direct influence on the TBB performance.

There are few studies (Mark et al., 2002) on the liquid phase aerobic biodegradation of isopropyl alcohol (IPA), the model pollutant used in the present work; to our knowledge there are no reports on its biodegradation on supported biofilm systems. It seems that IPA mineralization follow the path isopropyl alcohol $\rightarrow$ acetone $\rightarrow CO_2$.

In this paper we report on the hydrodynamics of a cocurrent down flow isopropanol-removing TBB. We study the effect of superficial liquid mass flow rate and bed void fraction on the liquid phase residence time distribution; gas-, liquid-, and gas-liquid pressure drop; dynamic and total liquid hold-up; and biofilm wetting efficiency. Finally, we discuss the TBB performance in relation to the magnitude of the main variables.

2. Materials and Methods

2.1 The trickle-bed bioreactor

Experiments were carried out in an acrylic TBB (0.143 m ID × 1.90 m of total length, of which only 1.6 m were packed with 316 SS 1.0 in Pall rings with a bed void fraction of 0.94). A schematic diagram of the TBB system is shown in Figure 1. The TBB consists of four 40 cm long identical modules, each supported on a SS grid. Below the three first modules there is a conical liquid redistribution plate. The TBB also has sampling ports al 0, 25, 50, 75 and 100 % of the total packed-bed length. A microbial consortium previously acclimatized for isopropyl alcohol (IPA) mineralization was used as the active biological phase (Cruz-Diaz, 2005). IPA-saturated air mixed with a second air flow was introduced at the top of the bioreactor; the flow of both streams were controlled by mass-flow controllers (Aalborg 0-5 and 0-100 LPM, USA). The liquid phase (mainly water with nutrients) was also fed to the top of the TBAB, where it was distributed over the top of TBB cross-sectional area by a liquid distributor (a nylon plate with 37 pieces of 316 SS tubing 0.25 in nominal ×1 in long). Gas and liquid contact exist prior to their entrance to the bed. Below the TBB there is a 16 L holding tank, from which the liquid is recirculated to the top of the TBB. The liquid pH was controlled by the addition of 1N HCl by a pH controller (Barnanat, USA). All gas and liquid lines were made of copper tubing.

2.2 Experiments

Five sets of experiments were performed, each corresponding to different stages of biomass growth as expressed in a specific bed void fraction (ε). The first set of experiments was performed with the packing without biomass. In the next three sets (ε=0.86, 0.70, 0.60) the biomass was of an aerobic nature. In the last set of experiments (ε=0.41, "clogging") the IPA removal took place mainly by an anaerobic route. During each set of experiments the bed void fraction was kept constant by means of a reduction of the nitrogen source in the liquid medium. In each set of

experiments, the superficial liquid mass flow rate (L) was varied to observe its effect on the hydrodynamic and biological parameters. The L values used for each experimental set were 6.8, 9.8, 11.8, and 13.8 kg/m^{2}s. The superficial gas mass velocity (G) was kept constant at 0.063 kg/m^{2}s for all experiments. These combinations of flows allowed the TBB to operate in the trickle flow regime, as defined in a flow regime map prepared by Gianetto and Specchia (1992).

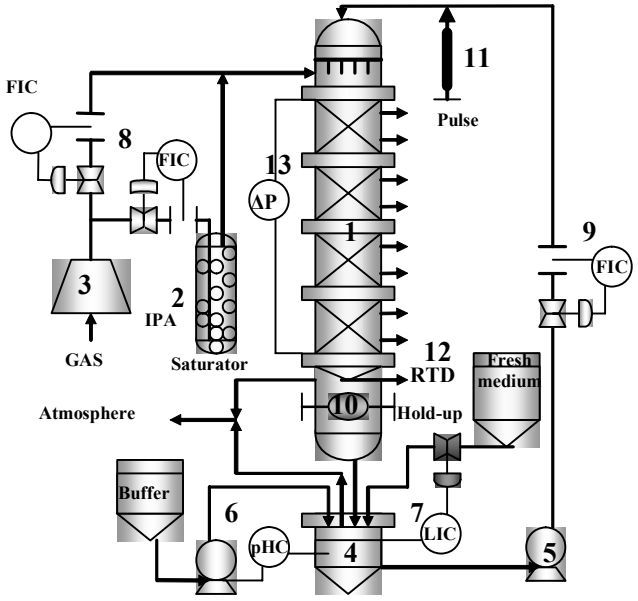

Figure 1. TBB system schematic diagram. 1-TBB. 2-saturator. 3-air compressor. 4-liquid holding tank. 5-liquid recirculation pump. 6-pH control system. 7-fresh liquid medium addition system. 8-air flow controllers. 9-liquid flow rotameter. 10-flood gate. 11-tracer injection port. 12-liquid sampling port for RTD determination. 13-manometer.

IPA inlet load to the TBB is shown in Table 1.

Table 1. IPA inlet load (g/m^{3}h)

	L (kg/m^{2}s)			
$\varepsilon \downarrow$	6.8	9.8	11.8	13.8
0.86	167.4	182.4	165.4	177.5
0.70	187.4	182.4	217.3	197.4
0.60	179.7	159.3	167.3	196.5
0.44	136.1	148.8	158.0	170.2

The TBB hydrodynamic characterization consisted of the determination of liquid residence time distributions (RTD) and mean liquid residence time, pressure drop, dynamic liquid hold-up, total liquid hold-up, and wetting efficiency. For the biological response the following parameters were determined: inlet and outlet IPA gas concentration, IPA and acetone liquid concentration, total IPA elimination

capacity, and CO_2 and methane production, expressed as a mineralization percentage. IPA and acetone in the gas and liquid phases, and CO_2 and methane in the gas were determined by gas chromatography. Experimental procedures and analytical methods are described elsewhere (Trejo-Aguilar et al., 2005; Cruz-Diaz, 2005).

3. Results and discussion

3.1 Liquid residence time distribution

Figures 2 to 5 show the experimental age distribution curves $E(\theta)$ as a function of dimensionless time for the five bed void fractions and the four liquid mass rates. The experimental data were fitted to the *N*-CSTR model (parameter: *N*) and to the analytical solutions of the dispersion model with open-open and closed-closed boundary conditions (parameter: Peclet number, $Pe_{(o\text{-}o)}$, $Pe_{(c\text{-}c)}$). The mean residence time (t_R) is also shown in the figures. It may be observed in these figures that the RTD for the packing without biomass there is some asymmetry (main peak to the left of the mean residence time) indicating a wall effects and channeling, which may be due to: (a) a too high packing to column diameter ratio ($d_p / d_{col} = 0.166$), which ideally should be between 0.1 to 0.125 (Seader and Henley, 1998); and (b) the geometry of the Pall ring packing which is "open" and does not correct liquid maldistribution, even though there are liquid redistribution plates between the packing modules of the TBB. It also may be observed that this tendency diminish somewhat as the liquid mass rate is increased.

For the experiments with *aerobic* biomass (ε = 0.86, 0.70, and 0.60) the biofilm formation on the packing surface helps correct liquid maldistribution, particularly at the higher liquid mass rates and lower bed void fractions. However, DTR data suggests that there is some stagnant zones (long tail and main peak before the mean residence time) and internal recirculation (secondary "humps").

When the bed void fraction was ε = 0.44, the biomass turned *anaerobic*, as indicated by the presence of methane and foul odor. At all liquid mass rates channeling is present, together with stagnant liquid zones and internal recirculation (humps on the right hand side of the DTR), particularly at the higher liquid mass rates. At 9.8 and 6.8 kg/m^{2}s DTR turn shorter and wider, indicating larger amounts of dispersion and higher deviations from plug flow. Stagnant zones and internal recirculation may be explained by the change in the biofilm density and structure, since it was observed that it turned dark and loose.

The characteristics of the present TBB may be approximated to those of a "clossed vessel", as discussed by Levenspiel (1999). The parameters of the dispersion model with closed-closed boundary conditions and large amounts of dispersion (D/uL>0.01) conditions are presented in Table 2, and were calculated by the procedure proposed by van der Laan (1958). In this table D/uL is the inverse of the Peclet number, D is the dispersion coefficient, u is liquid average velocity and L is the bed length.

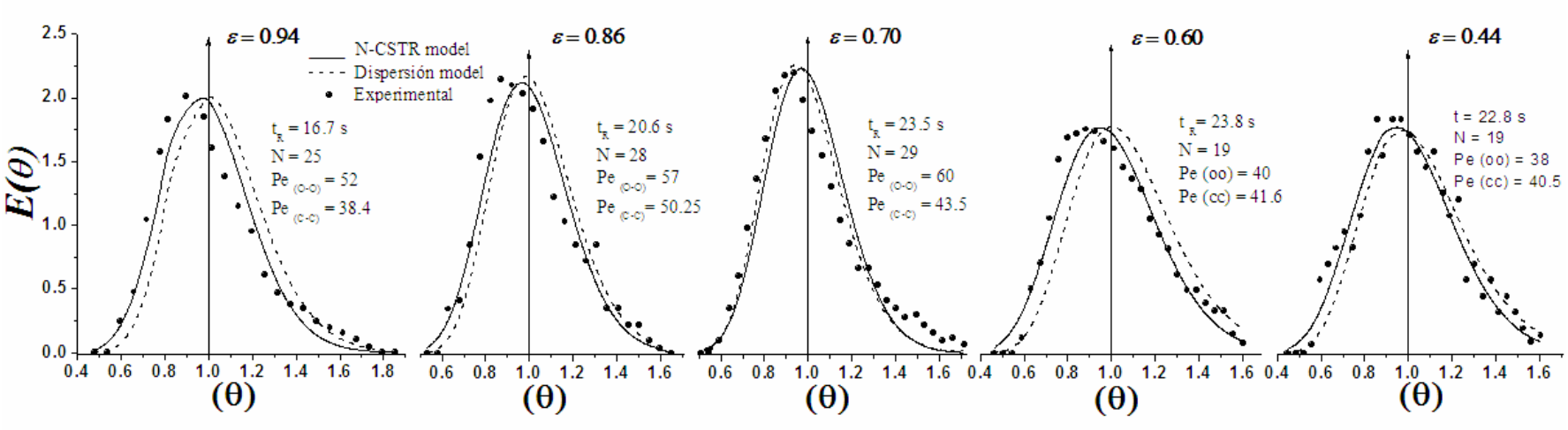

Figure 2. Liquid RTD for $L = 6.8\ \text{kg/m}^2 \cdot \text{s}$ and $G = 0.063\ \text{kg/m}^2 \cdot \text{s}$ at different stages of biomass growth (ε).

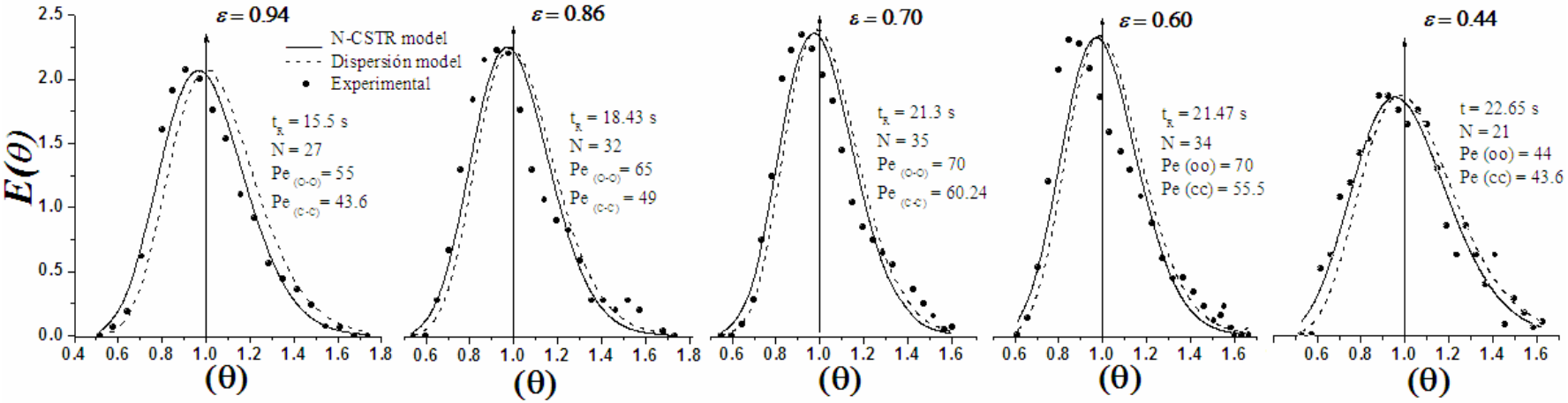

Figure 3. Liquid RTD for $L = 9.8\ \text{kg/m}^2 \cdot \text{s}$ and $G = 0.063\ \text{kg/m}^2 \cdot \text{s}$ at different stages of biomass growth (ε).

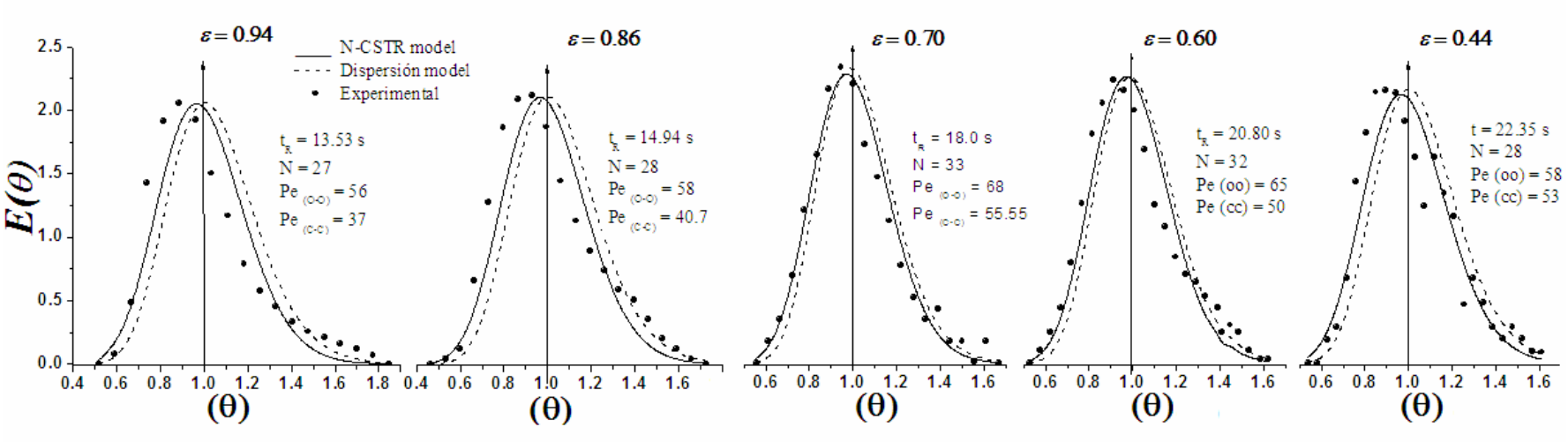

Figure 4. Liquid RTD for $L = 11.8\ \text{kg/m}^2 \cdot \text{s}$ and $G = 0.063\ \text{kg/m}^2 \cdot \text{s}$ at different stages of biomass growth (ε).

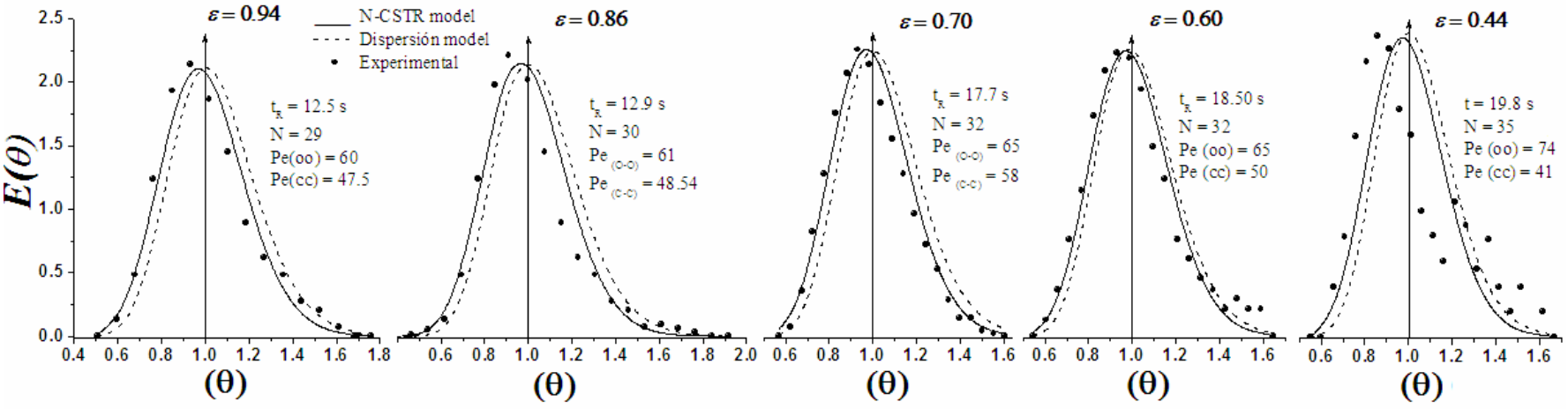

Figure 5. Liquid RTD for $L = 13.8\ \text{kg/m}^2 \cdot \text{s}$ and $G = 0.063\ \text{kg/m}^2 \cdot \text{s}$ at different stages of biomass growth (ε).

Table 2. Dispersion model parameters with closed-closed boundary conditions

	$D\times10^4$ (m^2/s)				D/uL				Variance σ_θ^2			
	L (kg/m^{2}s)											
$\varepsilon\downarrow$	6.8	9.8	11.8	13.8	6.8	9.8	11.8	13.8	6.8	9.8	11.8	13.8
0.94	3.0	3.8	5.5	5.3	0.026	0.023	0.028	0.021	0.050	0.045	0.054	0.041
0.86	2.5	3.7	5.4	5.6	0.020	0.020	0.025	0.020	0.039	0.040	0.048	0.041
0.70	3.6	3.7	4.8	5.7	0.023	0.017	0.018	0.017	0.045	0.033	0.036	0.033
0.60	4.4	4.7	6.3	7.8	0.024	0.018	0.020	0.020	0.047	0.038	0.039	0.039
0.44	5.7	8.2	8.1	1.3	0.023	0.023	0.019	0.024	0.044	0.045	0.037	0.047

This table shows that the smallest values of the model parameters for a liquid mass rate of 6.8 kg/m^{2}s are obtained at a bed void fraction of 0.86 and hence the smallest dispersion. For the liquid mass rates of 9.8, 11.8, and 13.8 kg/m^{2}s, this happens at a bed void fraction of 0.7. It may be said that biomass growth improves the flow pattern up to a point in which it begins again to deviate more and more from plug flow. Due to the complex and changing physical characteristics of the bed, the three parameter model represents better the flow pattern in a TBB, as shown by Cruz-Diaz et al.(2007).

3.2 Pressure drop

Gas pressure drop per unit bed length is shown in Figure 6, liquid-full bed pressure drop is depicted in Figure 7, and gas-liquid pressure drop appear in Figure 8.

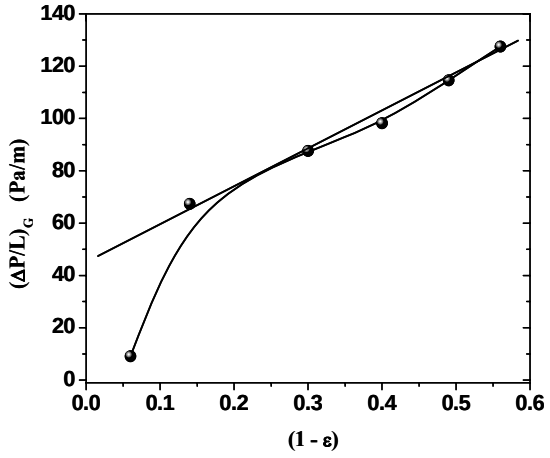

Figure 6. Gas phase pressure drop per unit length vs occupied bed fraction. G=0.063 kg/m^{2}s

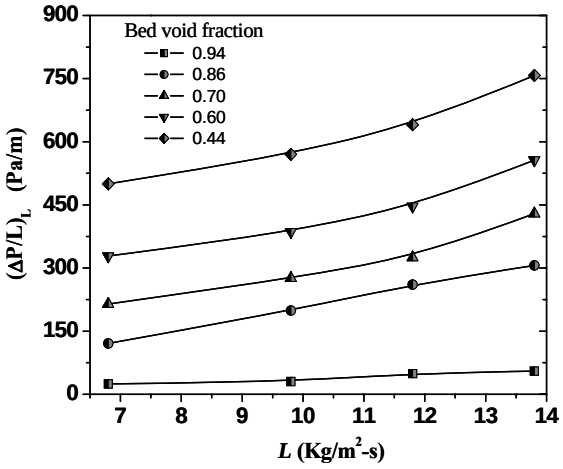

Figure 7. Liquid-full bed pressure drop per unit length as a function of liquid rate.

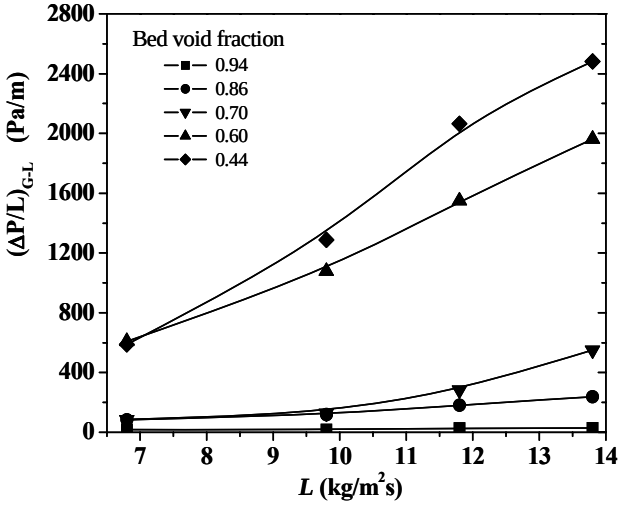

Figure 8. Gas-liquid pressure drop as a function of liquid rate. G=0.063 kg/m^{2}s

It may be seen in Figure 6 that the gas pressure drop increases sharply at the beginning of the biofilm formation and afterwards it increases linearly as bed void fraction is reduced as a consequence of continued biomass growth. Figure 7 shows that the liquid-full bed pressure drop increases slowly when there is no biomass present. When there is biomass present this pressure drop increases nearly proportionally with bed void fraction and with liquid mass rate, as expected. This pattern changes when there is gas and liquid flow present, as shown in Figure 8. In this case, for the bed void fraction values of 0.94, 0.86 y 0.70 the pressure drop increases slowly with liquid flow and then the increment is larger at higher liquid mass rates; when the bed void fraction increases to 0.6 and 0.44, there is a strong pressure drop increment for all liquid mass rates. It may be said that gas-liquid pressure drop goes through tree stages of growth; first, there is a lag phase, where at any liquid mass rate pressure drop increases slowly when biomass growth is relatively small; then, there is a sharp increment when biomass growth is large ($\varepsilon \approx 0.6$), and finally the rate of pressure drop growth starts to decline at ε=0.44, when the TBB is almost clogged due to excessive biomass growth.

Pressure drop data obtained in the present study are larger than those reported by Trejo-Aguilar et al (2005). In the later study the authors used an antifoaming agent due to the excessive foam formation in their system and thus the pressure drop was much lower than without the antifoaming agent. In the present study no antifoaming agent was used.

We attempted, with little success, to correlate our gas-liquid pressure drop data with several expressions developed for chemical trickle-bed reactors. Of the correlations developed for biofilters, only the equation developed by Deront et al. (1998) approximated partially the data at the early stages of biomass growth. Then, to date it is not possible yet to predict gas-liquid pressure drop in TBB with simple models. It may be necessary to use more complex models, such as the ones developed by Iliuta and Larachi (2005, 2006) to adequately describe pressure drop in TBB.

3.3 Liquid hold-up

Figures 9 and 10 show the total liquid hold-up and the dynamic liquid hold-up. Total liquid hold-up was calculated from the volumetric liquid mass rate and the mean residence time obtained from RTD. Figure 9 shows that total liquid hold-up increases with liquid mass rate and is larger at lower bed void fractions; its rate of growth decreases as the bed void fraction diminishes, but it is almost constant with respect to liquid mass rate. We correlated total liquid hold-up with following empirical power law model expression:

$$\varepsilon_L = \alpha L^{0.534} \tag{1}$$

In this equation ε_L is the total liquid hold up, L is the superficial liquid mass flow rate and α is a constant. It is interesting to point out that the resulting values of the parameter α are close to the average static liquid hold-up (see Table 2) for each bed void fraction. Equation (1) is plotted as the dashed line in Figure 9 and it has a 10 % relative error with respect the calculated values of total liquid hold-up.

The total liquid hold-up values reported here are somewhat smaller than those obtained by Trejo-Aguilar et al. (2005) at similar conditions. It should also be pointed out that these authors found a maximum in their total liquid hold-up data at a bed void fraction of 0.69, and then lower values at ε=0.41, a behavior not observed in the present study. These differences may be due to the nature of the biofilm formed, to the use of an antifoaming agent, and to the size of the Pall rings used as a support for the biofilm: while in the later study a 0.5 in packing was used, in the present case it was 1.0 in.

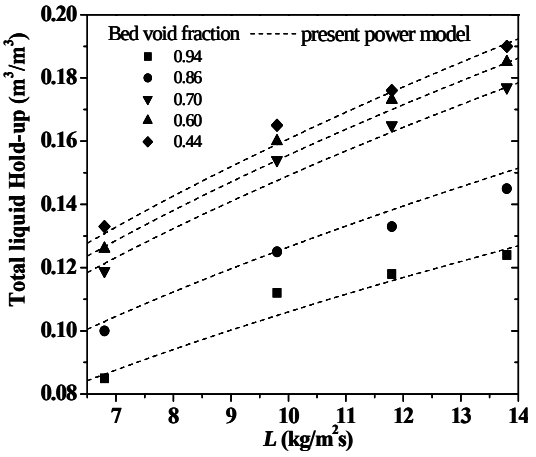

Figure 9. Total liquid hold-up as a function of liquid rate. G=0.063 kg/m^{2}s

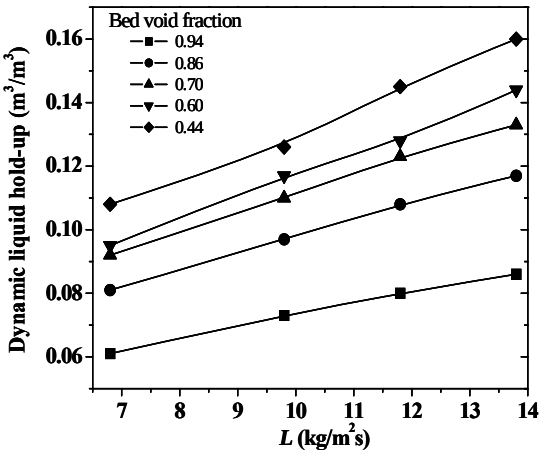

Figure 10. Dynamic liquid hold-up as a function of liquid rate. G=0.063 kg/m^{2}s

The experimental values of the dynamic liquid hold-up shown in Figure 10 approximately follow the same trends that the total liquid hold up, although their

magnitude is smaller, as expected: it increases with increasing liquid mass rate and with lower bed void fraction. We may speculate that the biomass present in the TBB has a capacity to loosely retain more liquid at higher liquid mass rates as it would a sponge; when the flow is stopped to measure the dynamic liquid hold-up, the retained liquid drains from the biofilm and it is accounted for as such.

Static liquid hold-up is defined as the difference between total and dynamic liquid hold-up. Table 3 shows the calculated values of the static liquid hold-up. It may be appreciated that it exhibits little variation with liquid mass rate and bed void fraction, as expected. The overall average value is 0.035.

Table 3. Static liquid hold-up values (m^3/m^3)

	L (kg/m^2s)			
$\varepsilon\downarrow$	6.8	9.8	11.8	13.8
0.94	0.026	0.039	0.038	0.036
0.86	0.023	0.035	0.032	0.033
0.70	0.029	0.046	0.042	0.044
0.60	0.027	0.043	0.041	0.041
0.44	0.025	0.039	0.031	0.030

3.4 Wetting efficiency

Wetting efficiency (f_w) is defined as the fraction of the total biofilm surface area that is wetted by flowing liquid. Since most substrate and oxygen mass transfer to the biofilm comes from the liquid, wetting efficiency is a very important parameter. This is especially true for the removal of IPA and other highly soluble VOC that are rapidly absorbed in the liquid phase. Wetting efficiency was estimated by means of a model developed by Pironti et al. (1999), which uses pressure drop, total liquid hold-up, and bed void fraction data. Pironti's equation is:

$$f_w = \frac{g\left[\rho_L \varepsilon_L + \rho_G\left(\varepsilon - \varepsilon_L\right)\right] - \varepsilon \rho_G g + \varepsilon\left[\left(\Delta P/L\right)_{GL} - \left(\Delta P/L\right)_G\right]}{\varepsilon g\left(\rho_L - \rho_G\right) + \varepsilon\left[\left(\Delta P/L\right)_L - \left(\Delta P/L\right)_G\right]} \tag{2}$$

where ρ_G and ρ_L are the gas and liquid densities, respectively; $\left(\Delta P/L\right)_{GL}$ is the pressure drop per unit length when both gas and liquid are flowing inside the TBB; $\left(\Delta P/L\right)_G$ is the pressure drop per unit length when only the gas flows; $\left(\Delta P/L\right)_L$ is the pressure drop per unit length when the bed is full of flowing liquid; ε is the bed void fraction; ε_L is the total liquid hold-up; and g is the acceleration due to gravity.

The calculated values of wetting efficiency are shown in Figure 11. It is evident that this parameter is larger when the liquid mass rate is high and when the bed void fraction is low. Such behavior may be explained by the reduction of the biofilm surface area as the bed void fraction is reduced and by the increment of the total liquid hold-up that occurs at those conditions. This is also consistent with the higher pressure drop observed at these conditions.

Since the wetting efficiency calculated by the Pironti model is strongly dependent on pressure drop, the values calculated in the present study at high liquid mass rates and low bed void fraction are about two times larger than those obtained by Trejo-Aguilar et al. (2005).

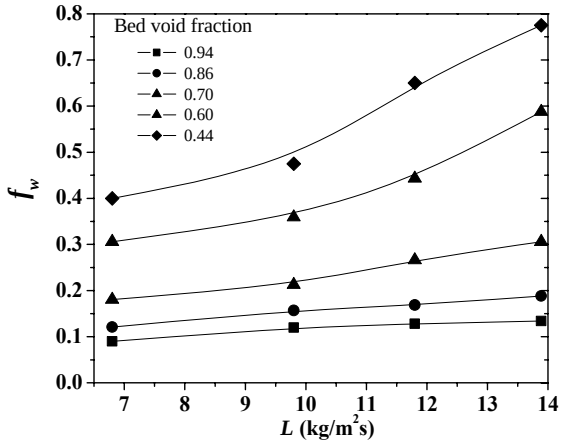

Figure 11. Wetting efficiency as a function of liquid mass rate.

3.5 TBB performance

The TBB capacity for IPA mineralization to CO_2 was affected by both liquid mass rate and bed void fraction, as shown in Figure 12 (IPA conversion to acetone is not discussed in this paper). It is evident that at low amounts of biomass (ε=0.86), the amount of carbon contained in IPA that was converted to CO_2 is between 21 and 27 %, and the higher value is obtained at the highest liquid mass rate, although this variable has a small effect. As biomass grows to give a bed void fraction of 0.70, The percentage converted to CO_2 grows somewhat to 32 % at the highest liquid mass rate; at this bed void fraction, the effect of liquid mass rate is more noticeable.

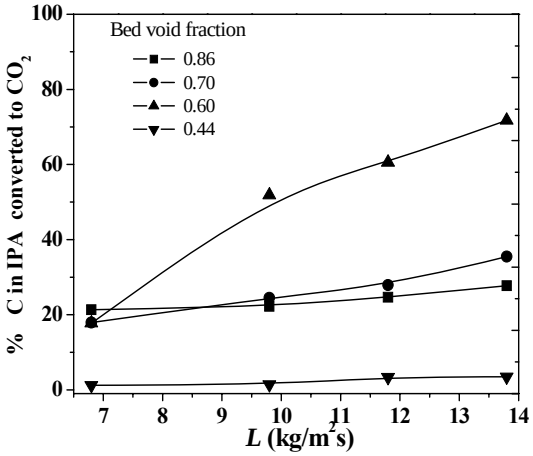

Figure 12. Carbon in IPA converted to CO_2 as a function of liquid mass rate.

The largest IPA conversion to CO_2 is reached at the bed void fraction of 0.60 and the effect of the liquid mass rate is very important: the highest conversion to CO_2 is obtained at the highest liquid mass rate. As the biomass grows to give a bed void fraction of 0.44, there is a dramatic decrease in the TBB capacity to mineralize IPA at any liquid mass rate.

As it will be discussed below, this behavior is due to the biomass transformation from aerobic to anaerobic. These results mean that to have a large IPA mineralization it is necessary to have a substantial amount of biomass and the use a high liquid mass rate, since a high liquid mass rate increases IPA mass transfer to the biofilm and improves its wetting efficiency. Additionally, it may be observed that for the lowest liquid mass rate of 6.8 kg/m^{2}s, the mineralization is about the same for the bed void fractions of 0.86, 0.70, and 0.60, probably due to poor wetting and low mass transfer rates to the biofilm.

The extent to which the biofilm present in the TBB is anaerobic may be inferred by the production of methane, as shown in Figure 13. It is clear there is no methane production when the bed void fractions are 0.86 and 0.70, and that its production starts when the bed void fraction is 0.60 and the liquid mass rates are 0.68 and 11.8 kg/m^{2}s. It also may be noted that even at this bed void fraction there is no methane production at the highest liquid mass rate of 13.8 kg/m^{2}s. Methane formation is a sign that not enough oxygen is being supplied to the biofilm deeper layers and thus the IPA biodegradation becomes oxygen limited to finally turn anaerobic.

At a bed void fraction of 0.44, the biofilm has lost almost all of its capacity to mineralize IPA and the production of methane is high, especially at the lower liquid mass rates. At this value of the bed void fraction, there has been a considerable reduction of biofilm surface area, and thus the supply of oxygen is also greatly reduced. It should be pointed out that the lower methane production observed at higher liquid mass rates does not resulted in increased mineralization to CO_2 (Figure 12) and thus it is likely that the biofilm irreversibly changed its nature.

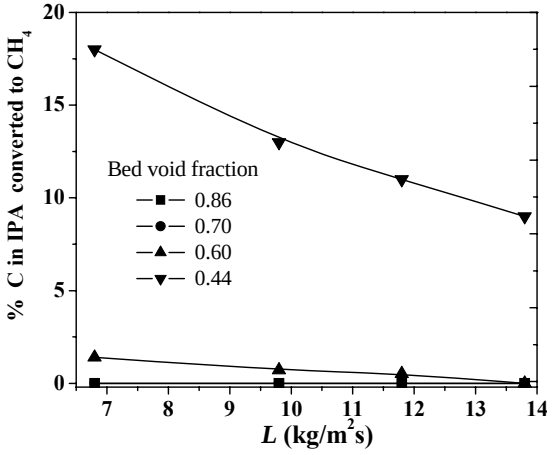

Figure 13. Carbon in IPA converted to methane as a function of liquid mass rate.

Since IPA is highly soluble, it is illustrative to examine the behavior of its concentration in the liquid phase (at the TBB liquid holding tank). It may be observed

in Figure 14 that the highest IPA liquid concentration occurs when the amount of biomass is smallest (ε=0.86), when the mineralization percentage is also lowest, and that it diminishes as liquid mass rate is increased. As bed void fraction grows to 0.7, IPA liquid concentration diminishes with liquid mass rate. The lowest IPA liquid concentration for all liquid mass rates is obtained at ε=0.60, when mineralization to CO_2 is largest. As void fraction continues to diminish to 0.44, IPA liquid concentration grows again, reflecting that the even though mineralization is rather small, a substantial amount of IPA is degraded by an anaerobic path. These data tends to show the consistency of the data shown in figures 12 and 13.

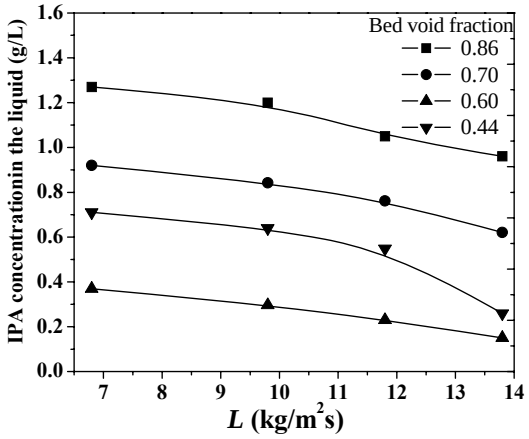

Figura12. Liquid phase isopropanol concentration as a function of liquid mass rate.

Conclusions

The hydrodynamics of a TBB which removes isopropyl alcohol has been experimentally studied, including the bioreactor performance with respect to liquid mass rate at different stages of biomass growth. Residence time distributions show that the liquid flow in the bioreactor deviates considerably from plug flow. Either the n-CSTR or the dispersion model represents fairly the liquid flow pattern at bed void fractions of 0.60 to 0.70 (moderate to medium biomass concentration); at bed void fraction of 0.44 (large biomass concentration), the TBB exhibits large channeling, stagnant zones, and internal recirculation. The resulting dispersion coefficients are in the order of 10^{-4} m^2/s. These results and those of Trejo-Aguilar et al. (2005) tend to show that plug flow is a poor assumption in TBB modeling.

Gas pressure drop grows linearly at low to medium bed void fraction and the sharply at bed void fraction of 0.44. Liquid-full bed pressure drop increases almost linearly with liquid mass rate and bed void fraction. Gas-liquid pressure drop is small up to a bed void 0.86 and is independent of liquid mass rate; at a bed void fraction of 0.70, gas-liquid pressure drop starts to increase with liquid mass rate. There is a sharp increase in gas-liquid pressure drop at bed void fraction of 0.60 and 0.44, and it shows linear dependence with liquid flow.

Total and dynamic hold-up follow the same trend, increasing with increased flow rate and diminishing bed void fraction. The former goes from around 0.08 at a liquid

mass rate of 6.8 kg/m^{2}s and no biomass present in the packing, to 0.19 at 13.8 kg/m^{2}s and a bed void fraction of 0.44. The later varies from 0.06 to 0.16 at the same conditions. A power law model for total liquid hold-up was developed and it describes well the experimental data. Static liquid hold-up varies little with liquid mass rate and bed void fraction; its overall average value of 0.035 which, interestingly enough, is the same average value of the packing without biomass.

Estimated wetting efficiency range from 0.1 when there is no biomass present and the liquid mass rate is 6.8 kg/m^{2}s to 0.8 when the bed void fraction is 0.44 and the liquid mass rate is 13.8 kg/m^{2}s. Pironti et al. (1999) method (and others) to estimate wetting efficiency are based on the assumption of a regular form packing and an even packing distribution in the bed, assumptions that hold only fairly for the biomass bed of a TBB. Thus, there is a need to develop correlations more appropriate for the physical characteristics of a TBB bed.

The largest isopropyl alcohol mineralization to CO_2 was 67.3 % and it was obtained at a liquid mass rate of 13.8 kg/m^{2}s and a bed void fraction of 0.60. At this bed void fraction mineralization grew with liquid mass rate. The lowest mineralization value was around 2 % and occurred at a bed void fraction of 0.44, when the biomass turned anaerobic. At this bed void fraction, the largest conversion to methane was 18 % when the liquid mass rate was 6.8 kg/m^{2}s. Overall, it was shown in this paper that the TBB performance is strongly dependent on hydrodynamics.

References

Cox, H., Deshusses M. 2002. Trickling biofilters for air pollution control. p. 782-795. Vol. 2. in G. Bitton (Editor-in-Chief), *The Encyclopedia of Environmental Microbiology*. Wiley. New York.

Cruz-Díaz. M. 2005. A hydrodynamic study of a trickle-bed bioreactor for the removal of isopropyl alcohol. MSc Thesis (in Spanish). Universidad Autónoma Metropolitana-Iztapalapa. Mexico.

Cruz-Diaz, M.R, Cabello, J., Lobo-Oehmichen, R. 2007. Liquid-phase residence time distribution in a trickle-bed biorreactor (in Spanish). Proceedings 29th AMIDIQ National Meeting. 1-4th May. Manzanillo. Mexico.

Deront, M., Samb F., Adler N., Peringer P. 1998. Biomass growth monitoring using pressure drop in a cocurrent biofilter. *Biotechnol. Bioeng.*, 60, 98-105.

Gianetto A., Specchia V. 1992. Trickle bed reactors: State of the art and perspectives. *Chem. Eng. Sci.*, 47, 3197-3213.

Iliuta, I., Larachi F. 2005.Modeling simultaneous biological clogging and physical plugging in trickle-bed bioreactors for wastewater treatment. 1. *Chem. Eng. Sci.*, 66, 1477–1489.

Iliuta, I., Larachi F. 2006. Dynamics of cells attachment, aggregation, growth and detachment in trickle-bed bioreactors. *Chem. Eng. Sci.*, 61, 4893 – 4908.

Levespiel, O. 1999. *Chemical Reaction Engineering.* 3rd Edition. Chap. 13. John Wiley. New York.

Lobo R., Revah S., Viveros, T. 1999. An analysis of a trickle-bed bioreactor: Carbon disulfide removal. *Biotechnol. Bioeng.*, 63: 98-109.

Mark, T.B., Vissanu, M., Phillip C.W. 2002. Kinetic analysis of high concentration isopropanol biodegradation by a solvent tolerant mixed microbial culture. *Biotechnol. Bioeng.* 78, 708-713.

Pironti F., Mizrahi D., Acosta A., Gonzalez-Mendizábal, D. 1999. Liquid-solid wetting factor in trickle-bed reactors: its determination by a physical method. *Chem. Eng. Sci.*, 54, 3793-3800.

Seader J.D., Henley J. E. 1998. *Separation Process Principles*. John Wiley. New York.

Trejo-Aguilar, G., Revah, S., Lobo-Oehmichen, R. 2005. Hydrodynamic characterization of a trickle bed air biofilter. *Chem. Eng. J.*, 113, 145-152.

van der Laan E.T. 1958. Letter to the Editor. *Chem. Eng. Sci.*, **7,** 187.

van Swaaij, W.P.M., Charpentier, J.C., Villermaux, J. 1969. Residence time distribution in the liquid phase of trickle flow in packed columns. *Chem. Eng. Sci*., 24, 1083-1095.